Catalysis Science & Technology

Accepted Manuscript

This article can be cited before page numbers have been issued, to do this please use: J. Tian, W. Chen, P. WU, Z. Zhu and X. Li, *Catal. Sci. Technol.*, 2018, DOI: 10.1039/C8CY00023A.

ROYAL SOCIETY OF CHEMISTRY

rsc.li/catalysis

View Article Online
DOI: 10.1039/C8CY00023A

Cu-Mg-Zr/SiO_2 Catalyst for Selective Hydrogenation of Ethylene Carbonate to Methanol and Ethylene Glycol

Jingxia Tian[a], Wei Chen[a], Peng Wu[a], Zhirong Zhu[b], Xiaohong Li[a,*]

[a] Shanghai Key Laboratory of Green Chemistry and Chemical Processes, School of Chemistry and Molecular Engineering, East China Normal University, 3663 North Zhongshan Rd., Shanghai 200062, China

[b] Department of Chemistry, Tongji University, 1239 Siping Road, Shanghai 200092, China

Corresponding author:

Xiaohong Li

Tel/Fax: +86-21-62238590

E-mail: xhli@chem.ecnu.edu.cn

View Article Online
DOI: 10.1039/C8CY00023A

Abstract: Cu_x-Mg_y-Zr_z/SiO_2 catalyst with a total metal loading of 60 wt.% prepared by a deposition-precipitation method was applied for selective hydrogenation of ethylene carbonate to methanol and ethylene glycol in a fixed-bed reactor. As a result, the Cu_8-Mg_1-$Zr_{0.47}/SiO_2$ catalyst furnished 99% of ethylene carbonate conversion with 85% of selectivity to methanol and 99% of selectivity to ethylene glycol under the optimized reaction conditions. Moreover, the Cu_8-Mg_1-$Zr_{0.47}/SiO_2$ catalyst also showed good lifetime and neither the activity nor selectivity decreased during 208 h test. The reaction was found to depend sensitively on the Cu particle size, the surface acidity and the catalyst surface composition. The synergistic effect between balanced Cu^0 and Cu^+ sites was considered to play a critical role in attaining high yields of methanol and ethylene glycol. The boric oxide also had a positive effect on the hydrogenation of ethylene carbonate, affording higher selectivity to methanol under much milder conditions.

Keywords: Selective hydrogenation; Cu_8-Mg_1-$Zr_{0.47}/SiO_2$ catalyst; Ethylene carbonate; Methanol; Ethylene glycol

View Article Online
DOI: 10.1039/C8CY00023A

1. Introduction

With increase of utilization of carbon-rich fossil fuels, the concentration of carbon dioxide in the atmosphere has significantly increased in the past century, which causes global environmental concern.[1-2] Therefore, transformation and utilization of CO_2 aroused more and more interests. In addition to attempts in reducing the CO_2 output, the utilization of CO_2 as a C_1 feedstock for carbon recycling to produce methanol (ME) becomes increasingly important. Although a lot of researches on the direct CO_2 hydrogenation to produce ME has been intensively made, relatively harsh conditions to achieve high catalytic efficiency and lower CO_2 conversion hinder the industrialization.[3-7] With Cu-based catalyst, which was commonly adopted for direct carbon dioxide hydrogenation to ME, the conversion only reached 20% with the selectivity to ME of 80% even at higher temperatures (250-300 ^oC).[8-15] Besides, some other transition metal and noble metal catalysts were also attempted such as Pb/SiO_2, $Au/TiO_2(ZnO)$, La_2O_3, $Li\text{-}Pb/SiO_2$, etc..[16-17] However, due to the thermodynamically stable and kinetically inert nature of the CO_2 molecules, high activation energy barriers have to be overcome for the cleavage of the C=O bonds in CO_2 .[18-19] Even under the harsh conditions, comparatively lower results, including 1%-30% CO_2 conversion with the selectivity to ME of 20%-90%, are usually furnished.[20-21] In general, it is still very difficult for the direct hydrogenation of carbon dioxide.

Nevertheless, carbon dioxide can be easily transformed to ethylene carbonate (EC) by reacting with ethylene epoxide.[22-23] It is a non-toxic, stable, cheap and an environmentally benign process. Moreover, hydrogenation of EC can also produce ME as well as ethylene glycol (EG) under much milder conditions (Scheme 1). Consequently, hydrogenation of EC can not only provide a new way for producing

View Article Online
DOI: 10.1039/C8CY00023A

ME, but also is an alternative approach for the indirect utilization of CO_2. Nonetheless, the hydrogenation of C=O group in EC remains challengeable due to the resonance stabilization effect of two adjacent alkoxyl groups.[24-25] Thus, only a few homogeneous catalyst systems have successfully realized the selective hydrogenation of EC with high efficiency.[26-28] As for the heterogeneous catalysts, the related reports are also mainly focused on Cu-based catalysts. In 2014, Li et al. firstly attempted the hydrogenation of EC over a heterogeneous copper-chromite nanocatalyst at 180 □ under 5 MPa of H_2, obtaining 60% selectivity to ME and 93% selectivity to EG.[29] Although the results are relatively lower, it demonstrates the feasibility for the hydrogenation of organic carbonates to ME over heterogeneous catalysts. However, the Cu-Cr catalyst system still suffers from low catalytic efficiency and the use of an environmentally unfriendly Cr-containing catalyst. Therefore, it is highly desirable to develop Cr-free heterogeneous catalysts for the efficient hydrogenation of EC.

Meanwhile, Liu et al. prepared the Cu/SiO_2 catalyst by a precipitation-gel method for the hydrogenation of EC. Although over 97% of selectivity to ME at about 99% of EC conversion was reported, longer reaction time, shorter catalyst lifetime, higher hydrogen pressure and too much catalyst dosage were adopted as a compromise.[30] Later, Chen et al. studied the EC hydrogenation with a Cu/HMS (hexagonal mesoporous silica) catalyst, with the selectivity to ME reaching 74% and the selectivity to EG over 99% with the EC conversion of 100%.[31] Very recently, Li et al. investigated the Cu/SBA-15 catalyst for EC hydrogenation, furnishing 62.3% of selectivity to ME and over 94.7% of selectivity to EG at the EC conversion of 100%.[32] More recently, Li et al. attempted the hydrogenation of EC over a heterogeneous Cu/SiO_2 prepared by an ammonia evaporation method at 180 □ and 5 MPa H_2, showing 70.8% of ME selectivity with 98% of selectivity to EG as well.[33]

View Article Online
DOI: 10.1039/C8CY00023A

Thus, there are still a series of problems to be solved for the selective hydrogenation of EC with a Cu-based catalyst. Higher ME selectivity is still anticipated with a much more active catalyst under much milder conditions. Additionally, the catalyst stability is also desired to be greatly improved for a Cu-based catalyst. Herein, we were motivated to modify the Cu/SiO_2 catalyst with the second and even the third component in order to significantly enhance the catalytic performance for the hydrogenation of EC. As a result, the Cu_8-Mg_1-$Zr_{0.47}/SiO_2$ catalyst with a total metal loading of 60 wt.% prepared via a precipitation-deposition method showed better behaviors toward the selective hydrogenation of EC under milder conditions.

2. Experimental

2.1 Chemicals

EC was purchased from Aladdin and used as received. $Cu(NO_3)_2{\cdot}3H_2O$, $Mg(NO_3)_2{\cdot}6H_2O$, $Zn(NO_3)_2{\cdot}6H_2O$, $Al(NO_3)_2{\cdot}9H_2O$, $Ce(NO_3)_3{\cdot}6H_2O$, KNO_3, $Zr(NO_3)_4{\cdot}5H_2O$, Na_2CO_3 and 1, 4-dioxane were purchased from Sinopharm Chemical Reagent Co, Ltd. and used as received as well.

2.2 Catalyst preparation

The Cu/SiO_2, $Cu\text{-}M/SiO_2$ or $Cu\text{-}Mg\text{-}Zr/SiO_2$ catalysts were prepared by a deposition-precipitation method. An aqueous solution containing $Cu(NO_3)_2$ or/and $Mg(NO_3)_2$ (or $Zn(NO_3)_2$ or $Al(NO_3)_2$, $Ce(NO_3)_3$ or KNO_3) with/without $Zr(NO_3)_4$ with different molar ratios was made and stirred for about 30 min at room temperature. Then, the above solution was transferred to a round-bottomed flask and a proper amount of SiO_2 was added. The total metal loading based on the final catalyst was set

View Article Online
DOI: 10.1039/C8CY00023A

to 60 wt.%. Then, the mixed solution was heated and maintained at 75 ^{o}C. After that, an aqueous solution of 7 wt.% Na_2CO_3 was added to adjust the solution pH value at about 7, and the mixture was stirred at 75 ^{o}C for additional 8 h. Finally, the resultant precipitate was recovered by filtration, washed with plenty of deionized water, and dried overnight at 110 ^{o}C. Subsequently, the samples were calcined at an elevated temperatures in static air for 5 h. In some cases, boric oxide with a loading of 0.5 wt.% was also impregnated to the as-calcined Cu-Mg-Zr/SiO_2 catalyst precursor to investigate the promotion effect of boric oxide. Then, the as-calcined samples were shaped and sieved to 20-40 meshes for use.

2.3 Catalyst characterization

The XRD patterns of samples were recorded on a Bruker D8 Advance X-ray diffractometer using Ni-filtered Cu Kα radiation (λ=1.5406 Å) with a scanning speed of 60^{o}/min with a voltage of 40 kV and a current of 40 mA. Prior to taking XRD patterns, the as-calcined samples were reduced in flowing hydrogen at 350 ^{o}C for 2 h. N_2 physisorption of samples was conducted on a Quantachrome Autosorb-1 system at liquid nitrogen temperature (-196 ^{o}C) after the samples were outgassed at 300 ^{o}C under vacuum for 3 h to remove physically adsorbed species. The specific surface areas were calculated by the Brunauer-Emmett-Teller (BET) equation. Total pore volumes were evaluated at relative pressures (P/P_0) close to unity. Pore size distributions were estimated by the Barrett-Joyner-Halenda (BJH) method according to the desorption branch of the isotherms. The transmission electron microscopy (TEM) images were recorded with an FEI Tecnai G2-TF30 electron microscope operated at an accelerating voltage of 300 kV.

The H_2-TPR (temperature-programmed reduction) was conducted with a

View Article Online
DOI: 10.1039/C8CY00023A

Micromeritics AutoChem II Chemisorption Analyzer. During the experiments, each sample (100 mg) was outgassed under flowing He (99.999%, 30 ml/min) at 450 ^{o}C for 60 min and then cooled to ambient temperature. The H_2-TPR profiles were obtained with a H_2 (99.999% purity, 30 ml/min) from 50 ^{o}C to 800 ^{o}C with a ramping rate of 10 ^{o}C/min.

NH_3-TPD (temperature-programmed desorption) measurements were carried out on a unit DAX-7000 instrument (Huasi Technology Co., Ltd, China). Before each measurement, the catalyst samples were pretreated at 450 ^{o}C under He flow (99.999%, 30 ml/min) for 1 h and then *in situ* reduced at different temperatures with 5% H_2-Ar for 2 h. Then, the reduced catalysts were exposed to a NH_3 flow (99.999%, 30 ml/min) at 80 ^{o}C for 1 h and then heated linearly from 80 to 1000 ^{o}C with a ramping a rate of 10 ^{o}C/min in a He flow (99.999%, ml/min). The desorbed NH_3 was on-line detected by a thermal conductivity detector (TCD), and the TCD signals were calibrated by a given volume of NH_3. The thermogravimetric (TG) analysis of the samples was conducted from r.t. to 1073 K under air atmosphere with a Mettler Toledo TGA/SDTA851^{e} apparatus. Before the TG experiments, the samples were pretreated as follows: 600 mg of as-calcined Cu/SiO_2 or Cu_8-Mg_1-$Zr_{0.47}/SiO_2$ was immersed into 4 ml of 1,4-dioxane solution containing 10 wt.% of EC for 2 h. Then, the samples were filtered and dried overnight at 80 ^{o}C. The TG experiments were performed in the range of 25-800 ^{o}C in air.

The IR spectra were measured on a Vertex 70 (Bruker) FT-IR spectrometer in the range of 400-4000 cm^{-1}. The sample powders were mixed with KBr (2 wt.%) and pressed into self-supported disks at room temperature. The X-ray photoelectron spectrum (XPS) of sample was recorded with ESCALAB 250 spectrometer with Al Kα X-ray radiation source (*hv*=1486.6 eV) operated at 14 kV and 20 mA. The

View Article Online
DOI: 10.1039/C8CY00023A

carbonaceous C1s line (284.6 eV) was used as the reference to calibrate the binding energies (BEs). The spectra shown in the figures have been corrected by subtraction of a Shirley background. Spectral fitting and peak integration was done using the XPSPEAK software.

2.4 Catalytic test

The selective hydrogenation of EC was performed using a fixed-bed reactor. Typically, 1.0 g of as-calcined catalyst precursor (20-40 meshes) was loaded into a stainless steel tubular reactor (with 55 cm of length and i.d. of 12 mm) with a thermocouple inserted into the catalyst bed for control of the actual temperature. The catalyst precursor was reduced *in situ* in a flowing hydrogen (99.999%, 2 MPa, 60 ml/min) at 350 ^{o}C for 4 h firstly. Then, the hydrogen flow rate was modulated using a mass flow controller and the pressure was controlled by a regulator valve. The hydrogenation of EC began after EC solution (dissolved in 1,4-dixoane) was pumped to the catalyst bed at a tunable flow rate. Normally, 0.02 ml/min of EC solution, 60 ml/min of hydrogen, 3 MPa of hydrogen at 180 ^{o}C were adopted for a standard catalytic test. For optimization of reaction parameters, effects of EC flow rate, hydrogen flow rate, hydrogen pressure and reaction temperatures on the hydrogenation of EC were also investigated individually.

The products were collected every 2 h and the samples collected after 4 h time of stream were analyzed offline using GC with an FID (TECHCOMP GC-7900 Plus, Tianmei Ltd. Co.). The response factor of each component was calculated using standard samples and was used to calculate the conversion and selectivity. For catalyst stability test, the reaction was performed continuously and the sample was collected every 2 or 3 h. The error bar for the catalytic testing is $\pm$ 5% based on GC analysis.

View Article Online
DOI: 10.1039/C8CY00023A

3 Results and discussion

3.1 Catalytic performance of Cu/SiO_2, Cu-M/SiO_2 and Cu-Mg-Zr/SiO_2 catalysts

Firstly, we investigated the Cu/SiO_2 catalyst for the hydrogenation of EC. As displayed in Fig. S1A, the Cu/SiO_2 catalyst afforded 99% of EC conversion with a 99% of selectivity to EG, however, only 30% of selectivity to ME was obtained with the Cu/SiO_2 catalyst. Although both the EC conversion and the selectivity to EG are quite high, the selectivity to ME was rather low compared with those reported in literature.[30-33] This may be due to that the Cu/SiO_2 prepared by a deposition-precipitation method had larger Cu particle size and the surface composition was not optimal for the selective hydrogenation of EC to ME in accompany with diol. Additionally, the reaction conditions were not optimized yet.

In order to improve the selectivity to ME, the second metal M was doped to Cu/SiO_2 catalyst with a Cu/M molar ratio of 7/1 and then applied to the hydrogenation of EC. As also displayed in Fig. S1A, the conversion of EC almost kept constant and reached over 90% with different Cu_7-M_1/SiO_2 catalysts. However, the selectivity to ME and EG varied with different Cu_7-M_1/SiO_2 catalysts. Only Mg doped Cu_7-Mg_1/SiO_2 catalyst exhibited the positive promotion effect and slightly increased the selectivity of ME to 34%. To our disappointment, other metals such as Al, Ce, Zn and K doped Cu/SiO_2 catalysts furnished inferior results to the Cu/SiO_2 catalyst, including selectivity to ME and EG. Among all the Cu_7-M_1/SiO_2 catalysts, the Cu_7-Zn_1/SiO_2 catalyst afforded the lowest EC conversion and selectivity to ME, while the Cu_7-Al_1/SiO_2 catalyst gave the lowest selectivity to EG.

In order to explain this phenomenon, the Cu_7-M_1/SiO_2 catalysts were characterized using XRD. All the supported Cu catalysts showed three obvious

View Article Online
DOI: 10.1039/C8CY00023A

diffraction peaks at 2θ of 43.3°, 50.4° and 74.1°, assignable to (111), (200) and (220) planes of Cu (Fig. S1B). Moreover, trace amount of CuO species were also detected for all catalysts, which might be originated from the unreduced CuO or from re-oxidation of Cu^0 particles when contacted air again after reduction. Because no protective step was taken to avoid surface oxidation after reduction of samples, we would not discuss the CuO diffraction anymore in the following studies and just concentrated on the diffraction of Cu(111) plane. Compared with other catalysts, the Cu_7-Mg_1/SiO_2 catalyst showed much stronger diffraction intensity of Cu(111) plane. According to the Scherrer equation, the average Cu crystallite size was about 21 nm, 30 nm and 31 nm for Cu/SiO_2, Cu_7-Mg_1/SiO_2 and Cu_7-K_1/SiO_2, respectively. The average Cu crystallite size was only about 11 nm for Cu_7-Zn_1/SiO_2, while for Cu_7-Al_1/SiO_2 and Cu_7-Ce_1/SiO_2, it was about 18 nm and 21 nm, respectively. On recalling the catalytic results obtained with Cu_7-M_1/SiO_2 catalysts, the Cu_7-Zn_1/SiO_2 and Cu_7-Al_1/SiO_2 catalysts with smaller Cu crystallite size gave the lower catalytic performance, while the Cu_7-Mg_1/SiO_2 catalyst with the largest Cu crystallite size afforded better results. This implies that the Cu particle size was not the only factor to influence the catalytic performance.

Although the selectivity to ME with the Cu_7-Mg_1/SiO_2 catalyst was slightly improved, the enhancement was very limited. In order to further enhance the catalytic performance, the Cu/Mg molar ratio *x* was optimized. As shown in Fig. S2A, the EC conversion and EG selectivity did not vary with different Cu/Mg molar ratios and almost kept constant at around 100%, while the selectivity to ME was significantly affected by the molar ratio of Cu/Mg. The selectivity to ME increased with Cu amount firstly and reached a maximum when *x* was equal to 8. When *x* was further

View Article Online
DOI: 10.1039/C8CY00023A

increased, the selectivity to ME was decreased instead. As a result, the highest selectivity to ME of 48% was obtained with the Cu_8-Mg_1/SiO_2 catalyst.

In order to understand the influence, the Cu_x-Mg_1/SiO_2 catalysts were characterized using XRD. For the Cu_x-Mg_1/SiO_2 catalysts, the Cu(111) diffraction became stronger with the increase of *x* value (Fig. S2B). According to the Scherrer equation, the average Cu crystallite size was about 26 nm for $Cu_{6.5}$-Mg_1/SiO_2, while it was about 30 nm for Cu_7-Mg_1/SiO_2. The Cu_8-Mg_1/SiO_2 catalyst showed the broadest diffraction peak of Cu(111) plane, with the average Cu crystallite size of about 23 nm, indicating that the Cu particles were more uniformly and highly dispersed. If *x* value was further increased to 9, the Cu(111) diffraction became stronger again and the average Cu crystallite size was about 26 nm. Therefore, Cu/Mg molar ratio was set as 8 in the following studies.

To further improve the catalytic ability, the third component Zr with trace amount was added to Cu_8-Mg_1/SiO_2 and applied to the EC hydrogenation. Fig. S3A shows the detailed reaction results. The selectivity to ME with the Cu_8-Mg_1-Zr_z/SiO_2 catalysts was influenced greatly by the molar ratio of Cu/Mg/Zr (8/1/z), whereas EC conversion and EG selectivity almost kept constant. Similarly, the selectivity of ME was increased with Zr amount initially and reached a maximum at the Cu/Mg/Zr molar ratio of 8/1/0.47. If the Zr amount was further increased, the selectivity to ME with the Cu_8-Mg_1-Zr_z/SiO_2 catalyst was dramatically decreased. As a result, the Cu_8-Mg_1-$Zr_{0.47}/SiO_2$ catalyst furnished the highest selectivity to ME of 65%.

For understanding these behaviors, the Cu_8-Mg_1-Zr_z/SiO_2 catalysts were characterized using XRD firstly (Fig. S3B). After doping of Zr with trace amount, the average Cu crystallite size decreased significantly, which indicates that the Cu particle dispersion was obviously improved. Moreover, the diffraction of Cu(111) became

View Article Online
DOI: 10.1039/C8CY00023A

weaker with increase of Zr amount and then became slightly stronger with further increase of Zr amount. According to the Scherrer equation, the average Cu crystallite size was about 11 nm for Cu_8-Mg_1-$Zr_{0.44}$/SiO_2 and Cu_8-Mg_1-$Zr_{0.50}$/SiO_2, whereas it was about 14 nm of Cu_8-Mg_1-$Zr_{0.48}$/SiO_2, and the Cu_8-Mg_1-$Zr_{0.47}$/SiO_2 had the smallest average Cu crystallite size of about 10 nm. Among the Cu_8-Mg_1-Zr_z/SiO_2 catalysts, the Cu_8-Mg_1-$Zr_{0.47}$/SiO_2 catalyst showed the highest selectivity to ME, probably due to that it had the smallest Cu crystallite size. However, there are maybe some other influencing factors except the Cu particle size to affect the catalytic performance of the Cu_8-Mg_1-Zr_z/SiO_2 catalysts, which need to be clarified through detailed characterizations.

Moreover, in order to compare the promotion effect of Mg or Zr alone on the Cu/SiO_2 catalyst for the EC selective hydrogenation reaction, the Cu-Zr binary catalyst with a molar ratio of 8/0.47, just as the same as that in the Cu_8-Mg_1-$Zr_{0.47}$/SiO_2 catalyst, was prepared and investigated in the hydrogenation of EC. As clearly displayed in Fig 1A, the Cu_8-$Zr_{0.47}$/SiO_2 catalyst also showed full conversion of EC, accompanied with nearly 100% selectivity of EG. Moreover, the Cu_8-$Zr_{0.47}$/SiO_2 catalyst gave slightly higher ME selectivity compared with Cu/SiO_2 and Cu_8-Mg_1/SiO_2 catalysts as well. Nevertheless, the ternary Cu_8-Mg_1-$Zr_{0.47}$/SiO_2 catalyst was the most selective one among the Cu/SiO_2 catalysts. According to the Scherrer equation, the average Cu crystallite size for the Cu/SiO_2 catalysts is as follows: Cu/SiO_2 > Cu_8-Mg_1/SiO_2 > Cu_8-$Zr_{0.47}$/SiO_2 > Cu_8-Mg_1-$Zr_{0.47}$/SiO_2 (Fig. 1B).

3.2 Characterization of supported Cu catalysts

In order to understand the promotion effect of Mg and Zr additives on the Cu/SiO_2 catalysts for the hydrogenation of EC, the Cu/SiO_2, Cu_8-Mg_1/SiO_2,

View Article Online
DOI: 10.1039/C8CY00023A

Cu_8-$Zr_{0.47}/SiO_2$ and Cu_8-Mg_1-$Zr_{0.47}/SiO_2$ catalysts were thoroughly characterized using N_2 sorption, TEM, H_2-TPR, XPS, NH_3-TPD, IR, etc.

Firstly, the as-calcined Cu/SiO_2, Cu_8-Mg_1/SiO_2 and Cu_8-Mg_1-$Zr_{0.47}/SiO_2$ catalysts were characterized using nitrogen sorption. As shown in Fig. 2, all catalysts displayed type IV isotherms with hysteresis loops at comparatively higher relative pressure, indicating that all the catalysts had relatively large mesopores. Obviously, the Cu_8-Mg_1-$Zr_{0.47}/SiO_2$ catalyst had larger BET specific surface area compared with Cu/SiO_2 and Cu_8-Mg_1/SiO_2 catalysts. For clarity, Table 1 lists the detailed physicochemical parameters of relevant samples. The BET specific surface area of SiO_2 was about 202 m^2/g. With loading of 60 wt.% Cu or Cu-Mg or Cu-Mg-Zr, the specific surface area calculated using per g of catalyst was remarkably decreased, mainly due to that the specific surface area was mainly contributed by the support while its weight was only 40% in the resultant catalyst. In order to compare the influencing effect of different metals on the specific surface area of SiO_2 support, the BET specific surface area for different Cu/SiO_2 catalysts was also calculated per g of SiO_2. As a result, after loading Cu, the Cu/SiO_2 had a BET specific surface area of 180 m^2/g_{SiO2}. If Mg was further doped, the BET specific surface area of the Cu_8-Mg_1/SiO_2 was further declined to 140 m^2/g_{SiO2}. However, after Zr was also added, the BET specific surface area of the Cu_8-Mg_1-$Zr_{0.47}/SiO_2$ was increased to 205 m^2/g_{SiO2} instead. Compared with SiO_2 support itself, the specific surface area of Cu/SiO_2 and Cu_8-Mg_1/SiO_2 catalysts was distinctly decreased, but the specific surface area of Cu_8-Mg_1-$Zr_{0.47}/SiO_2$ was almost equal to that of SiO_2 support. This indicates that doping of Zr with optimal amount is helpful for the dispersion of Cu particles, in good agreement with the XRD results.

To further demonstrate the influence of particle size and dispersion on catalytic

View Article Online
DOI: 10.1039/C8CY00023A

activity, the relevant supported Cu catalysts were also characterized by TEM (Fig. 3). The Cu particles were more uniformly dispersed after Mg or Zr was doped compared with those in Cu/SiO_2 catalyst. Moreover, the Cu_8-Mg_1-$Zr_{0.47}/SiO_2$ catalyst showed more uniform Cu particle dispersion and less aggregation. According to the Cu particle size distribution in Fig. 3B, D, F and H, the average Cu particle size was about 7 nm for the Cu/SiO_2 catalyst and Cu_8-Mg_1/SiO_2 catalyst. The average Cu particle size was about 6.8 nm and 5.6 nm for the Cu_8-$Zr_{0.47}/SiO_2$ catalyst and Cu_8-Mg_1-$Zr_{0.47}/SiO_2$ catalyst, respectively. These results are in good accordance with the XRD and nitrogen sorption results. It is confirmed again that after doping of Mg and Zr to the Cu/SiO_2 catalyst, sintering or aggregation of Cu particles could be effectively prevented due to the significant interaction of Cu-Mg-Zr.

According to literature, there would have a strong interaction between Cu particles and SiO_2 if copper phyllosilicate species can be formed during preparation. Subsequently, reduction of copper phyllosilicate can form Cu^+ species easily, while further reduction of Cu^+ species derived from copper phyllosilicate needs much higher temperature.[34-36, 29] To examine whether copper phyllosilicate existed in this case, some relevant samples were characterized using IR spectroscopy. As shown in Fig. 4, the formation of copper phyllosilicate was confirmed by the appearance of the δ_{OH} band at 665 cm^{-1} and the ν_{SiO} shoulder peak at about 1100 cm^{-1} in the calcined samples. The relative amount of copper phyllosilicate in the as-calcined Cu_8-Mg_1-$Zr_{0.47}/SiO_2$ was calculated by considering the integrated intensity of the δ_{OH} band at 665 cm^{-1} normalized to the integrated intensity of the ν_{SiO} symmetric stretching band of SiO_2 at 800 cm^{-1} in terms of I_{665}/I_{800}. It is worthwhile to note that the I_{665}/I_{800} ratio only gives a qualitative estimation of the amount of copper phyllosilicate, because the extinction coefficients of the corresponding IR bands are

View Article Online
DOI: 10.1039/C8CY00023A

not known. Consequently, there are copper phyllosilicate species in Cu/SiO_2, Cu_8-Mg_1/SiO_2 and Cu_8-Mg_1-$Zr_{0.47}/SiO_2$ catalysts. The I_{665}/I_{800} value is about 0.18, 0.25 and 0.44 for Cu/SiO_2, Cu_8-Mg_1/SiO_2 and Cu_8-Mg_1-$Zr_{0.47}/SiO_2$, respectively. Among the three samples, the Cu_8-Mg_1-$Zr_{0.47}/SiO_2$ had the most copper phyllosilicate species, so we can deduce that the Cu^+ species derived from copper phyllosilicate would be more than that in the other two catalysts.

Furthermore, the Cu/SiO_2, Cu_8-Mg_1/SiO_2 and Cu_8-Mg_1-$Zr_{0.47}/SiO_2$ were also characterized by H_2-TPR to investigate the metal-support interaction and the interaction between different metal species (Fig. 5). For the as-calcined Cu/SiO_2, the H_2 uptake initiated from 100 ^oC and ended at about 240 ^oC. The reduction started from 115 ^oC and ended at about 275 ^oC for the as-calcined Cu_8-Mg_1/SiO_2, about 30 ^oC higher than that for the as-calcined Cu/SiO_2. For the as-calcined Cu_8-Mg_1-$Zr_{0.47}/SiO_2$ catalyst precursor, the reduction started from 135 ^oC and stopped at about 300 ^oC. Undoubtedly, the hydrogen uptake during 100 to 300 ^oC was assignable to reduction of CuO or copper phyllosilicate to Cu^+ or Cu^0.[37-38] Compared with Cu/SiO_2, the Cu_8-Mg_1/SiO_2 and Cu_8-Mg_1-$Zr_{0.47}/SiO_2$ precursors need to be reduced at higher temperatures. This suggests that with addition of more dopants into Cu/SiO_2 catalyst, the interaction between Cu and Mg or Zr additives became stronger. As a result, the as-calcined Cu_8-Mg_1-$Zr_{0.47}/SiO_2$ catalyst precursor needed to be reduced at the highest temperature.

In order to determine the surface properties of the catalysts, the related Cu catalysts were also characterized using X-ray photoelectron spectroscopy. As can be seen from Fig. 6A, for all the Cu/SiO_2, Cu_8-Mg_1/SiO_2, Cu_8-$Zr_{0.47}/SiO_2$ and Cu_8-Mg_1-$Zr_{0.47}/SiO_2$ catalysts, the Cu2p 3/2 was centered at 932.5 eV, while the Cu2p 1/2 was centered as 952.4 eV, characteristic of Cu^0 or Cu^+ species. The satellite peak

View Article Online
DOI: 10.1039/C8CY00023A

at around 945-950 eV and 960-965 eV is also observed, probably due to re-oxidation of the reduced catalysts. As the binding energy for Cu^0 and Cu^+ species is too close to distinguish, the Cu LMM Auger electron spectroscopy was adopted. Based on the systematic studies on the Cu-based catalysts in literature, the balanced Cu^+/Cu^0 proportion is considered as the key factor for the polarization of C=O bond and the activation of H_2.[35,39] Fig. 6B shows the Cu LMM Auger electron spectra for Cu/SiO_2, Cu_8-Mg_1/SiO_2, Cu_8-$Zr_{0.47}/SiO_2$ and Cu_8-Mg_1-$Zr_{0.47}/SiO_2$ catalysts. All the spectra were deconvoluted to four peaks using Lorenz/Gaussian of 1/99.[33, 38, 40-45] The peaks at 568.0 eV are assigned to Cu^0 species, while the peak at 570.0 eV is attributed to Cu^+ species. Due to overlapping of Cu^0 and Cu^+ peaks at around 570-574 eV, we calculated the $Cu^+/(Cu^0+Cu^+)$ just according to peak intensity at 568.0 eV and 570.0 eV. As already attached in Fig. 6B, the intensity ratio of surface $Cu^+/(Cu^+ + Cu^0)$ for the Cu/SiO_2, Cu_8-Mg_1/SiO_2, Cu_8-$Zr_{0.47}/SiO_2$ and Cu_8-Mg_1-$Zr_{0.47}/SiO_2$ catalysts was 65.9%, 70.7%, 66.9% and 70.1%, respectively. Note that an optimal amount of Cu^+ was observed on the surface of Cu_8-Mg_1-$Zr_{0.47}/SiO_2$ catalyst.

Moreover, the electronic state of the dopant Mg and Zr was also probed by the X-ray photoelectron spectroscopy. As displayed in Fig. 6C and D for Mg1s and Zr3d XPS spectra of the relevant catalysts, both Mg and Zr are in their oxidation states.

On recalling the catalytic results obtained with different Cu catalysts for the EC hydrogenation, the selectivity to ME with the Cu_8-Mg_1-$Zr_{0.47}/SiO_2$ catalyst was the highest among the three catalysts. It has been suggested that Cu^0 species adsorb dissociated H_2 and facilitate the hydrogenation and/or hydrogenolysis reactions, while Cu^+ sites act as electrophilic or Lewis acidic sites to polarize the carbonyl groups via the electron lone pair in oxygen.[46-47] A recent study by Scotti et al. reported that the Lewis acidity of CuO/SiO_2 catalyst was profoundly increased by the reduction of the

View Article Online
DOI: 10.1039/C8CY00023A

dispersed CuO phase to the metallic state.[48] In addition, due to the higher electron affinity of silicon, the electropositive copper species (Cu^{+}) strongly interacting with the surface of SiO_2 are reported to have strong Lewis acidity.[49] In this case, the XRD patterns showed the presence of dispersed Cu^0 species after reduction at 350 ^oC (Fig. S1B, Fig. S2B), while XPS results also proved the presence of Cu^+ on the surface. Therefore, the synergistic cooperation of Cu^0 and Cu^+ sites with optimized Cu^0/Cu^+ ratio played a critical role for the efficient hydrogenation of EC to ME and EG. Thus, we can conclude that the superior performance of the Cu_8-Mg_1-$Zr_{0.47}/SiO_2$ catalyst was attributed to the optimal $Cu^+/(Cu^+ + Cu^0)$ proportion.

In addition, the amount of Mg^{2+} and Zr^{4+} dopant were demonstrated to have profound influence on the evolution of textural and structural properties, the functionality of active phases and the catalytic behavior of the as-synthesized ternary catalysts (Cu, Mg^{2+} and Zr^{4+}). We can see from the TEM, H_2-TPR and Cu LMM that Mg^{2+} doped Cu_8-Mg_1/SiO_2 catalysts causes the reduction in the number of surface active Cu^0 sites and the activity of the Cu/SiO_2 based catalyst. But the Zr^{4+} further doped nanoscale Cu_8-Mg_1-$Zr_{0.47}/SiO_2$ catalyst was found to be helpful for enhanced Cu dispersion and a decreased amount of active surface Cu^+ sites, which promoted catalytic activity in EC hydrogenation to EG and ME effectively. [50] Alternatively, Mg^{2+} and Zr^{4+} dopant with oxidation state might be helpful for the adsorption and activation of EC, so that the bond cleavage and hydrogenation could be accelerated.

In order to clarify this issue, the Cu/SiO_2 and Cu_8-Mg_1-$Zr_{0.47}/SiO_2$ catalysts after immersed in the 1,4-dioxane solution containing EC for 2 h were characterized using TG technique under the ambient conditions. According to the TG profiles in Fig. 7, more weight loss was detected on the Cu_8-Mg_1-$Zr_{0.47}/SiO_2$, indicating that more EC was adsorbed on the Cu_8-Mg_1-$Zr_{0.47}/SiO_2$ surface than that on the Cu/SiO_2 surface. In

View Article Online
DOI: 10.1039/C8CY00023A

another word, the dopant Mg and Zr in oxidation states are helpful for the adsorption and activation of EC. Correspondingly, we also proposed a hypothesis for EC adsorption and activation and thus the hydrogenation to ME and EG (Fig. 8).

3.3 Optimization of reaction conditions

Based on the results obtained above, we found that the selectivity to ME was the highest with the Cu_8-Mg_1-$Zr_{0.47}/SiO_2$ catalyst. To discover the best performance of the Cu_8-Mg_1-$Zr_{0.47}/SiO_2$ catalyst to the greatest extent, the reaction parameters were optimized subsequently.

Firstly, the calcination temperature for Cu_8-Mg_1-$Zr_{0.47}/SiO_2$ catalyst precursor was changed in the range of 350 ^oC to 550 ^oC. As can be seen in Fig. S4, either decreasing the calcination temperature from 450 ^oC to 350 ^oC or increasing from 450 ^oC to 550 ^oC for the Cu_8-Mg_1-$Zr_{0.47}/SiO_2$ catalyst precursor, the selectivity of ME obtained with the resultant Cu_8-Mg_1-$Zr_{0.47}/SiO_2$ catalyst decreased obviously although the EC conversion and EG selectivity could keep almost constant.

To investigate the effect of reduction temperature, the Cu_8-Mg_1-$Zr_{0.47}/SiO_2$ catalyst reduced at different temperatures in the range of 300-450 ^oC was studied. As shown in Fig. S5A, decreasing or increasing the reduction temperature for the Cu_8-Mg_1-$Zr_{0.47}/SiO_2$ catalyst precursor, the selectivity to ME was declined. Remarkably, the Cu_8-Mg_1-$Zr_{0.47}/SiO_2$ catalyst after reduced at 350 ^oC showed the striking catalytic performance by comparison with those reduced at other temperatures. In order to explain the phenomenon, the Cu_8-Mg_1-$Zr_{0.47}/SiO_2$ catalysts after reduced at different temperatures were also characterized by XRD and NH_3-TPD. Clearly, the Cu_8-Mg_1-$Zr_{0.47}/SiO_2$ catalyst reduced at 350 ^oC showed slightly weaker Cu(111) diffraction and had comparatively smaller Cu particle size (Fig. S5B).

View Article Online
DOI: 10.1039/C8CY00023A

The NH_3-TPD curves for the Cu_8-Mg_1-$Zr_{0.47}/SiO_2$ catalysts after reduced at different temperatures are shown in Fig. S6. For all the Cu_8-Mg_1-$Zr_{0.47}/SiO_2$ catalysts reduced at different temperatures, only ammonia desorption at around 200 ^oC was detected, demonstrating that there are only weak acid sites on the Cu_8-Mg_1-$Zr_{0.47}/SiO_2$ catalysts despite of the reduction temperature. After quantitative calculation, the acid concentration is about 47.3 μmol g^{-1} for the one reduced at 300 ^oC. It is slightly decreased to 45.6 μmol g^{-1} for the one reduced at 350 ^oC. If the reduction temperature was further increased, the acid concentration was further decreased. As a result, the acid concentration was about 20 μmol g^{-1} when the reduction temperature was above 400 ^oC. This indicates that the appropriate acid amount is beneficial to the selectivity of ME.

In addition, the EC hydrogenation was carried out at different temperatures ranging from 160 ^oC to 200 ^oC. Fig. S7 exhibits the EC hydrogenation results obtained at different temperatures. Apparently, selectivity to ME and EG are greatly influenced by the reaction temperature. The selectivity to ME was dramatically decreased from 65% to 25% and the selectivity of EG declined from 99% to 68% when the reaction temperature was decreased from 180 ^oC to 160 ^oC. Of particular note is that the conversion of EC could be kept unchanged. However, when the reaction temperature was increased from 180 ^oC to 200 ^oC, the selectivity to ME and EG was declined too. It should be noted that EC hydrogenation is exothermic (ΔH = -71.59 kJ/mol) and thermodynamically favorable (ΔG = -25.62 kJ/mol), therefore, EC hydrogenation is more favorable at lower temperatures; while higher temperatures will facilitate the deep hydrogenation of EG to ethanol or a series of other side reactions.[32]

Besides, the flow rate of hydrogen and hydrogen pressure were also optimized in

View Article Online
DOI: 10.1039/C8CY00023A

detail. Hydrogen is used as a reactant in the reaction, so the hydrogen pressure might have a great impact on the catalytic performance. When hydrogen pressure was increased from 2 MPa to 3.0 MPa, the selectivity of ME was increased markedly from 48% to 65% (Fig. S8A). There was also a big increase in the selectivity to ME from 65% to 82% when the hydrogen pressure was further increased to 4.0 MPa. This demonstrates that higher pressure hydrogen is beneficial to increase the associatively adsorbed hydrogen atoms on the catalyst surface, so that the EC hydrogenation can be accelerated in accompany with promoted ME production. Moreover, when hydrogen flow was increased from 40 ml/min to 60 ml/min, the selectivity of ME was increased from 50% to 65% and the conversion of EC was increased from 75% to 99% as well (Fig. S8B). However, further increase of hydrogen flow rate cannot increase the selectivity of ME and the conversion of EC anymore. As for the $WHSV_{EC}$, the selectivity to ME was obviously decreased when $WHSV_{EC}$ was increased due to shorter contact time (Fig. S8C).

3.4 Catalyst life

The catalyst life is often investigated to evaluate the stability of the catalyst. As revealed in Fig. 9A, about 98% of EC conversion and EG selectivity was achieved with the fresh Cu_8-Mg_1-$Zr_{0.47}/SiO_2$ catalyst. With the reaction going, the conversion of EC and the selectivity of EG was gradually increased to 99% and can be kept almost constant. The selectivity to ME was about 65% under 3.0 MPa of H_2 pressure. If the hydrogen pressure was increased to 4.0 MPa, the selectivity to ME reached 82% and then kept almost constant. Within 208 h test, the conversion of EC, selectivity of ME and EG did not decrease, indicating that the catalyst had excellent stability. After the life test, the used catalyst was characterized using TG and as a result, no coke was

View Article Online
DOI: 10.1039/C8CY00023A

formed on the catalyst surface under the tested conditions. The used catalyst was also characterized using XRD. As shown in Fig. 9B, the copper particles hardly aggregate during 208 h test.

3.5 Effect of boric oxide

According to the literature,[30, 43, 51-52] when the catalyst was modified with boric oxide, the catalytic performance could be significantly improved. In this study, we also modified the Cu_8-Mg_1-$Zr_{0.47}$/SiO_2 catalyst with boric oxide with 0.5 wt.% and then submitted the modified Cu_8-Mg_1-$Zr_{0.47}$/SiO_2 catalyst to the EC hydrogenation. As displayed in Fig. 10, although the EC conversion and EG selectivity kept unchanged, the selectivity to ME was greatly increased to 80% with the Cu_8-Mg_1-$Zr_{0.47}$-0.5B/SiO_2 catalyst even under the hydrogen pressure of 3.0 MPa. Nevertheless, if more boric oxide was added, the catalytic performance was obviously decreased. When the hydrogen pressure was increased to 4.0 MPa (Fig. 10B), the selectivity to ME was further slightly increased to 85% with the Cu_8-Mg_1-$Zr_{0.47}$-0.5B/SiO_2 catalyst.

In order to understand the boric oxide promotion effect, the Cu_8-Mg_1-$Zr_{0.47}$-0.5B/SiO_2 catalyst was also characterized using TEM, H_2-TPR and XPS. As already displayed in Fig. 3I and J, the average Cu particle size of the Cu_8-Mg_1-$Zr_{0.47}$-0.5B/SiO_2 catalyst is about 5.7 nm, suggesting that the Cu particles are more uniform than other related Cu/SiO_2 catalysts. From Fig. 5, the reduction of the as-calcined Cu_8-Mg_1-$Zr_{0.47}$-0.5B/SiO_2 catalyst further shifted to higher temperature, indicating the interaction of Cu with additives became much stronger. This agrees well with the literature that the positive effect of boric oxide was

View Article Online
DOI: 10.1039/C8CY00023A

attributed to its relatively high affinity for electrons, which tends to lower the reducibility of the Cu^+ species.[43] Of particular note is that the Cu_8-Mg_1-$Zr_{0.47}$-0.5B/SiO_2 catalyst had the optimal surface $Cu^+/(Cu^+ + Cu^0)$ ratio (Fig. 6B). When we make a correlation between surface $Cu^+/(Cu^+ + Cu^0)$ ratio and the selectivity to ME, it is obvious that the optimal surface $Cu^+/(Cu^+ + Cu^0)$ ratio would lead to high selectivity to ME (Fig. 11B). Similarly, the correlation between Cu particle size and the selectivity to ME also showed a volcano-like curve (Fig. 11 A). In another word, the Cu_8-Mg_1-$Zr_{0.47}$-0.5B/SiO_2 catalyst had the optimal Cu particle size and the optimal surface $Cu^+/(Cu^+ + Cu^0)$ ratio so that the highest selectivity to ME was afforded.

4. Conclusions

The Cu-based catalysts with a total metal loading of 60 wt.% were applied for the hydrogenation of EC to ME and EG in a fixed-bed reactor. After screening different metal component, the ternary Cu-Mg-Zr/SiO_2 catalyst was found to be most active and selective for the tested reaction. Correspondingly, Cu/Mg/Zr molar ratio, calcination temperature and reaction parameters were optimized in detail. Nearly full conversion of EC conversion, over 99% EG selectivity and 85% selectivity to ME were achieved on the Cu_8-Mg_1-$Zr_{0.47}$/SiO_2 catalyst under the optimized reaction conditions. With the promotion of boric oxide, the selectivity to ME can be further improved. The Cu_8-Mg_1-$Zr_{0.47}$/SiO_2 catalyst also showed excellent stability during 208 h life test. Based on the detailed characterizations using XRD, N_2 sorption, TEM, H_2-TPR, NH_3-TPD, IR and XPS, the optimal $Cu^+/(Cu^0 + Cu^+)$ proportion on the Cu_8-Mg_1-$Zr_{0.47}$/SiO_2 catalyst surface, together with high specific surface area,

View Article Online
DOI: 10.1039/C8CY00023A

relatively smaller Cu crystallite size and optimal acid concentration played key roles in superior performance of the Cu_8-Mg_1-$Zr_{0.47}$/SiO_2 catalyst.

Conflicts of interest

There are no conflicts of interest to declare.

Acknowledgements

This work was supported by the National Natural Science Foundation of China (21273076 and 21373089), the Open Research Fund of Top Key Discipline of Chemistry in Zhejiang Provincial Colleges and Key Laboratory of the Ministry of Education for Catalysis Materials (Zhejiang Normal University) (ZJHX2013), and Shanghai Leading Academic Discipline Project (B409).

References

[1] M. Meinshausen, N. Meinshausen, W. Hare, S. C. B. Raper, K. Frieler, R. Knutti, D. J. Frame and M. R. Allen, Nature, 2009, 458, 1158-1162.

[2] A. Goeppert, M. Czaun, J. P. Jones, G. K. Surya Prakash, G. A. Olah, Chem. Soc. Rev. 2014, 43, 7995-8048.

[3] L. Wen, J. Li, J. Chem. Eng., 2008, 29, 33-37.

[4] Y. Fan, S. Wu, Chem. Ind. Eng. Prog., 2016, 35, 159-166.

[5] C. Wu, Y. Zhou, Z. Zou, Chin. J. Catal., 2011, 32, 1565-1572.

[6] H. Chen, Y. Liang, B. Wang, Chem. Ind. Eng. Prog., 2009, 28, 271-278.

[7] J. Ma, N. Sun, X. Zhang, N. Zhao, F. Xiao, W. Wei, Y. Sun, Catal. Today, 2009, 148, 221-231.

[8] T. Witoon, J. Chalorngtham, P. Dumrongbunditkul, M. Chareonpanich, J.

View Article Online
DOI: 10.1039/C8CY00023A

Limtrakul, Chem. Eng. J., 2016, 293, 327-336.

[9] Z. Zuo, L. Wang, P. Hai, W. Huang, Appl. Surf. Sci., 2014, 290, 398-404.

[10] K. Larmier, W. C. Liao, S. Tada, E. Lam, R. Verel, A. Bansode, A. Urakawa, A. Comas-Vives, C. Coperet, Angew. Chem. Int. Ed., 2017, 56, 2318-2323.

[11] M. Jia, W. Gao, H. Wang, Y. Wang, Chem. Ind. Eng. Prog., 2015, 34, 407-412.

[12] Z. Tan, W. Gao, H. Wang, C. Han, W. Guo, Chem. Ind. Eng. Prog., 2013, 32, 820-823.

[13] F. Liao, Z. Zeng, C. Eley, Q. Lu, X. Hong, S. C. E. Tsang, Angew. Chem. Int. Ed., 2012, 51, 5832-5836.

[14] F. Arena, K. Barbera, J. Italiano, G. Bonura, L. Spadaro, F. Frusteri, J. Catal., 2007, 249, 185-194.

[15] J. Słoczynski, R. Grabowski, P. Olszewski, A. Kozłowska, J. Stoch, M. Lachowska, J. Skrzypek, Appl. Catal. A, 2006, 310, 127-137.

[16] J. Wang, G. Li, Z. Li, C. Tang, Z. Feng, H. An, H. Liu, T. Liu, C. Li, Sci. Adv., 2017, 3, 1-10.

[17] J. Słoczynski, R. Grabowski, A. Kozłowska, P. Olszewski, M. Lachowska, J. Skrzypek, J. Stoch, Appl. Catal. A, 2003, 249, 129-138.

[18] A. M. Appel, J. E. Bercaw, A. B. Bocarsly, H. Dobbek, D. L. DuBois, M. Dupuis, J. G. Ferry, E. Fujita, R. Hille, P. J. A. Kenis, C. A. Kerfeld, R. H. Morris, C. H. F. Peden, A. R. Portis, S. W. Ragsdale, T. B. Rauchfuss, J. N. H. Reek, L. C. Seefeldt, R. K. Thauer, G. L. Waldrop, Chem. Rev., 2013, 113, 6621-6658.

[19] W. Wang, S. Wang, X. Ma, J. Gong, Chem. Soc. Rev., 2011, 40, 3703-3727.

[20] Y. Hartadi, D. Widmann, R. J. Behm, ChemSusChem, 2014, 8, 456-465.

[21] J. Wang, G. Li, Z. Li, C. Tang, Z. Feng, H. An, H. Liu, T. Liu, C. Li, Sci. Adv., 2017, 3, e1701290.

View Article Online
DOI: 10.1039/C8CY00023A

[22] Q. Wu, T. Ren, Chin. J. Chem. Eng., 2012, 12, 302-309.

[23] X. Lu, R. He, C. X. Bai, J. Mol. Catal. A, 2002, 186, 1-11.

[24] M. Ito, T. Ootsuka, R. Watari, A. Shiibashi, A. Himizu, T. Ikariya, J. Am. Chem. Soc., 2011, 133, 4240-4242.

[25] P. A. Dub, T. Ikariya, ACS. Catal., 2012, 2, 1718-1741.

[26] Z. Han, L. Rong, J. Wu, L. Zhang, Z. Wang, K. Ding, Angew. Chem. Int. Ed., 2012, 51, 13041-13045.

[27] E. Balaraman, C. Gunanathan, J. Zhang, L. J. W. Shimon, D. Milstein, Nat. Chem., 2011, 3, 609-614.

[28] T. Vom Stein, M. Meuresch, D. Limper, M. Schmitz, M. Hölscher, J. Coetzee, D. J. Cole-Hamilton, J. Klankermayer, W. Leitner, J. Am. Chem. Soc., 2014, 136, 13217-13225.

[29] C. Lian, F. Ren, Y. Liu, G. Zhao, Y. Ji, H. Rong, W. Jia, L. Ma, H. Lu, D. Wang, Y. Li, Chem. Commun., 2015, 51, 1252-1254.

[30] H. Liu, Z. Huang, Z. Han, K. Ding, H. Liu, C. Xia, J. Chen, Green Chem., 2015, 17, 4281-4290.

[31] X. Chen, Y. Cui, C. Wen, B. Wang, W-L. Dai, Chem. Commun., 2015, 51, 13776-13778.

[32] F. Li, L. Wang, X. Han, P. He, Y. Cao, H. Li, RSC Adv., 2016, 6, 45894-45906.

[33] F. Li, L. Wang, X. Han, Y. Cao, P. He, H. Li, Int. J. Hydrogen Energy, 2017, 42, 2144-2156.

[34] L.-F. Chen, P.-J. Guo, M.-H. Qiao, S.-R. Yan, H.-X. Li, W. Shen, H.-L. Xu, K.-N. Fan, J. Catal., 2008, 257, 172-180.

[35] J. Gong, H. Yue, Y. Zhao, S. Zhao, L. Zhao, J. Lv, S. Wang, X. Ma, J. Am. Chem. Soc., 2012, 134, 13922-13925.

View Article Online
DOI: 10.1039/C8CY00023A

[36] T. Toupance, M. Kermmarec, J.F. Lambert, C. Louis, J. Phys. Chem. B, 2002, 106, 2277-2286.

[37] Z. Li, G. Xu, H. Wang, H. Chen, Chin. J. Catal., 1995, 16, 10-14.

[38] J. Tian, J. Hu, W. Shan, P. Wu, X. Li, Appl. Catal. A, 2017, 544, 108-115.

[39] C. Wen, Y. Cui, X. Chen, B. Zong, W.-L. Dai, Appl. Catal. B, 2015, 162, 483-493.

[40] X. Huang, M. Ma, S. Miao, Y. Zheng, M. Chen, W. Shen, Appl. Catal. A, 2017, 531, 79-88.

[41] Z. Lu, H. Yin, A. Wang, J. Hu, W. Xue, H. Yin, S. Liu, J. Ind. Eng. Chem., 2016, 37, 208-215.

[42] T. Ghodselahi, M. A. Vesaghi, A. Shafiekhani, A. Baghizadeh, M. Lameii, Appl. Surf. Sci., 2008, 255, 2730-2734.

[43] Z. He, H. Liu, P. He, Y. Yuan, J. Catal., 2011, 277, 54-63.

[44] M. C. Biesinger, L. W. M. Lau, A. R. Gerson, R. S. T. Smart, Appl. Surf. Sci., 2010, 257, 887-898.

[45] Y. Cui, W-L. Dai, Catal. Sci. Technol., 2016, 6, 7752-7762.

[46] A. Yin, X. Guo, W-L. Dai, K. Fan, J. Phys. Chem. C, 2009, 113, 11003-11013.

[47] Y. Zhu, X. Kong, S. Zhu, F. Dong, H. Zheng, Y. Zhu, Y. Li, Appl. Catal. B, 2015, 166, 551-559.

[48] N. Scotti, M. Dangate, A. Gervasini, C. Evangelisti, N. Ravasio, F. Zaccheria, ACS Catal., 2014, 4, 2818-2826.

[49] Y. Zhu, Y. Zhu, G. Ding, S. Zhu, H. Zheng, Y. Li, Appl. Catal. A, 2013, 468, 296-304.

[50] X. Kong, Z. Chen, Y. Wu, R. Wang, J. Chen, L. Ding. RSC. Adv, 2017, 7, 49548-49561.

View Article Online
DOI: 10.1039/C8CY00023A

[51] S. Zhu, X. Gao, Y. Zhu, Y. Zhu, H. Zheng, T. Li, J. Catal., 2013, 303, 70-79.

[52] S. Zhao, H. Yue, Y. Zhao, B. Wang, Y. Geng, J. Lv, S. Wang, J. Gong, J. Catal., 2013, 297, 142-150.

View Article Online
DOI: 10.1039/C8CY00023A

Table 1. The phyicochemical parameters of SiO_2, as-calcined Cu/SiO_2, Cu_8-Mg_1/SiO_2 and Cu_8-Mg_1-$Zr_{0.47}/SiO_2$ catalysts.

Sample	S_{BET} ($m^2/g_{cat.}$)	S_{BET} (m^2/g_{SiO2})	V_p (cm^3/g)	D (nm)
SiO_2	202	202	1.12	27.3
Cu/SiO_2	72	180	0.90	20.2
Cu_8-Mg_1/SiO_2	56	140	0.98	27.2
Cu_8-Mg_1-$Zr_{0.47}/SiO_2$	82	205	1.20	27.4

View Article Online
DOI: 10.1039/C8CY00023A

Scheme and Figure captions

Scheme 1. Selective hydrogenation of ethylene carbonate to methanol and ethylene glycol.

Fig. 1. (A) The conversion of EC, the selectivity to EG and ME with Cu/SiO_2, Cu_8-Mg_1/SiO_2, Cu_8-$Zr_{0.47}/SiO_2$ and Cu_8-Mg_1-$Zr_{0.47}/SiO_2$ catalysts. Reaction conditions: 1 g of the as-calcined Cu catalyst precursor *in situ* reduced at 350 ^oC in 2.0 MPa H_2; Reaction temp. = 180 ^oC, H_2= 60 ml/min, $GHSV_{H2}$=2400, $WHSV_{EC}$ = 0.13, 3.0 MPa of H_2. (B) The XRD patterns of the Cu/SiO_2, Cu_8-Mg_1/SiO_2, Cu_8-$Zr_{0.47}/SiO_2$ and Cu_8-Mg_1-$Zr_{0.47}/SiO_2$catalysts.

Fig. 2. N_2 adsorption-desorption isotherms of SiO_2, as-calcined Cu/SiO_2, Cu_8-Mg_1/SiO_2 and Cu_8-Mg_1-$Zr_{0.47}/SiO_2$ catalysts.

Fig. 3. TEM images of (A) Cu/SiO_2, (C) Cu_8-Mg_1/SiO_2, (E) Cu_8-$Zr_{0.47}/SiO_2$, (G) Cu_8-Mg_1-$Zr_{0.47}/SiO_2$ and (I) Cu_8-Mg_1-$Zr_{0.47}$-0.5B/SiO_2 catalysts and the Cu particle size distribution of (B) Cu/SiO_2, (D) Cu_8-Mg_1/SiO_2, (F) $Cu_8Zr_{0.47}/SiO_2$, (H) Cu_8-Mg_1-$Zr_{0.47}/SiO_2$ and (J) Cu_8-Mg_1-$Zr_{0.47}$-0.5B/SiO_2.

Fig. 4. IR spectra of the as-calcined Cu/SiO_2, Cu_8-Mg_1/SiO_2 and Cu_8-Mg_1-$Zr_{0.47}/SiO_2$. The I_{665}/I_{800} intensity ratio represents the relative amount of copper phyllosilicate in the precursors.

Fig. 5. H_2-TPR profiles of the as-calcined Cu/SiO_2, Cu_8-Mg_1/SiO_2, Cu_8-Mg_1-$Zr_{0.47}/SiO_2$ and Cu_8-Mg_1-$Zr_{0.47}$-0.5B/SiO_2.

Fig. 6. (A) Cu 2p XPS spectra and (B) Cu LMM Auger electron spectra of Cu/SiO_2, Cu_8-Mg_1/SiO_2, Cu_8-$Zr_{0.47}/SiO_2$, Cu_8-Mg_1-$Zr_{0.47}/SiO_2$ and Cu_8-Mg_1-$Zr_{0.47}$-0.5B/SiO_2 catalysts, (C) Mg 1s XPS spectra and (D) Zr3d XPS spectra of the related Cu catalysts.

View Article Online
DOI: 10.1039/C8CY00023A

Fig. 7. The thermogravimetric curves of Cu/SiO_2 and Cu_8-Mg_1-$Zr_{0.47}/SiO_2$ catalysts after immersed in a 1,4-dioxane solution containing EC for 2 h.

Fig. 8. The hypothesis for EC activation and hydrogenation to ME and EG on the Cu_8-Mg_1-$Zr_{0.47}/SiO_2$ catalyst.

Fig. 9. (A) The conversion of EC, selectivity to ME and EG versus time on stream obtained with the Cu_8-Mg_1-$Zr_{0.47}/SiO_2$ catalyst. The reaction parameters are identical with those for Fig. 1 except the hydrogen pressure; (B) XRD patterns of the Cu_8-Mg_1-$Zr_{0.47}/SiO_2$ catalyst before and after use.

Fig. 10. Effect of boric oxide on EC hydrogenation under (A) 3.0 MPa of H_2, (B) 4.0 MPa of H_2. Other reaction parameters are identical with those for Fig. 1.

Fig. 11. (A) The correlation of ME selectivity and Cu particle size and (B) the correlation of ME selectivity and surface $Cu^+/(Cu^+ + Cu^0)$ ratio for the Cu/SiO_2, Cu_8-Mg_1/SiO_2, Cu_8-$Zr_{0.47}/SiO_2$, Cu_8-Mg_1-$Zr_{0.47}/SiO_2$ and Cu_8-Mg_1-$Zr_{0.47}$-$0.5B/SiO_2$ catalysts.

View Article Online
DOI: 10.1039/C8CY00023A

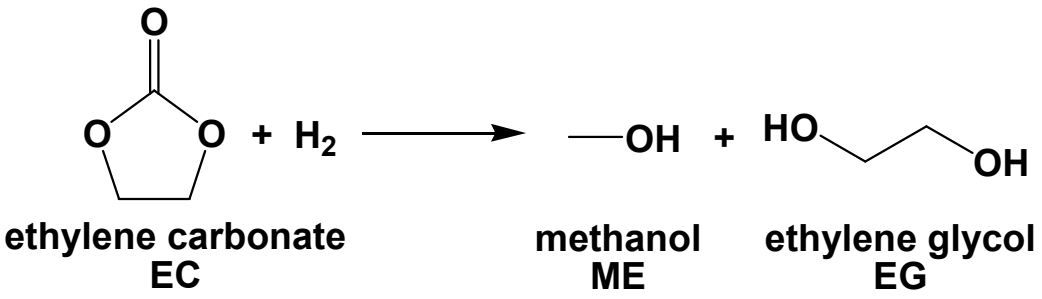

Scheme 1. Selective hydrogenation of ethylene carbonate to methanol and ethylene glycol.

View Article Online
DOI: 10.1039/C8CY00023A

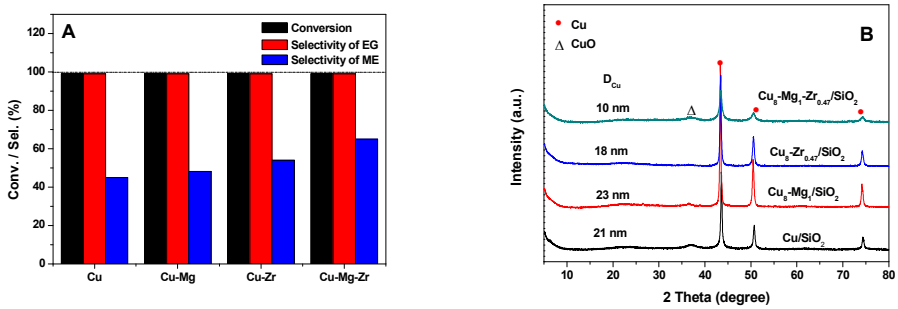

Fig. 1

View Article Online
DOI: 10.1039/C8CY00023A

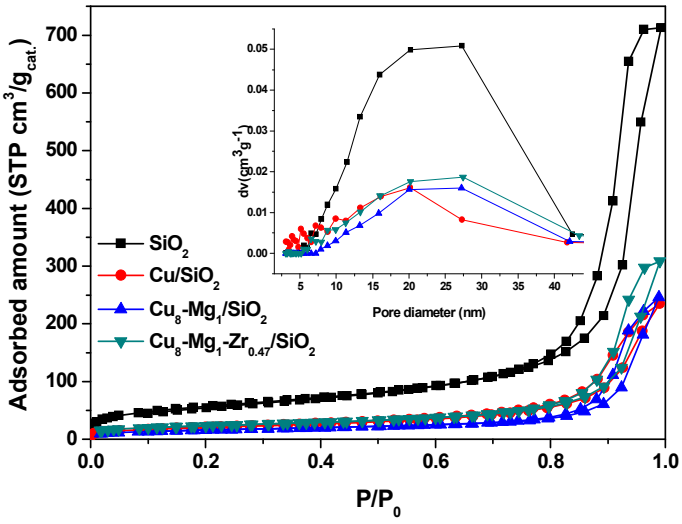

Fig. 2

View Article Online
DOI: 10.1039/C8CY00023A

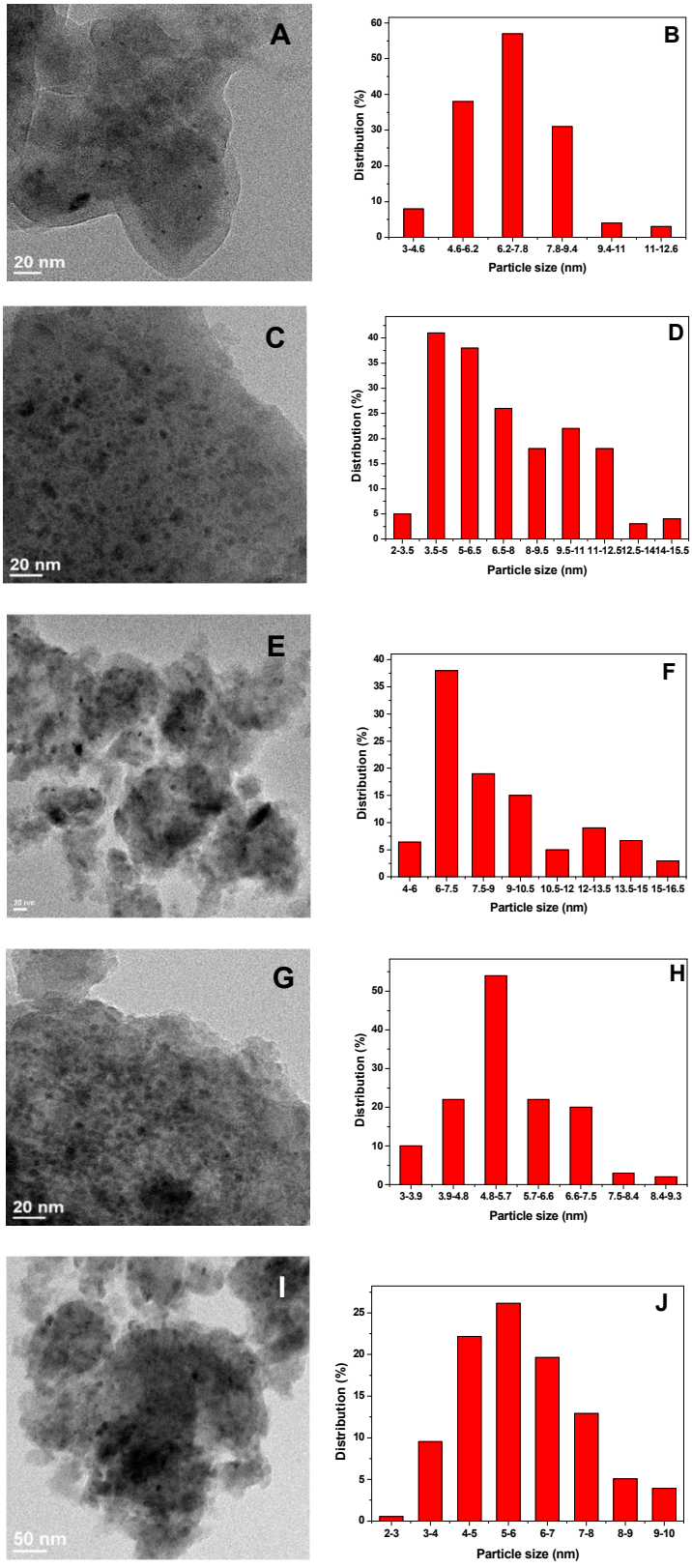

Fig. 3

View Article Online
DOI: 10.1039/C8CY00023A

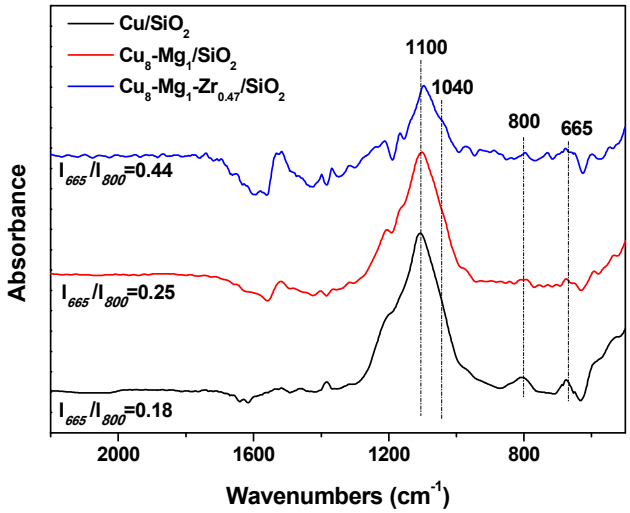

Fig. 4

View Article Online
DOI: 10.1039/C8CY00023A

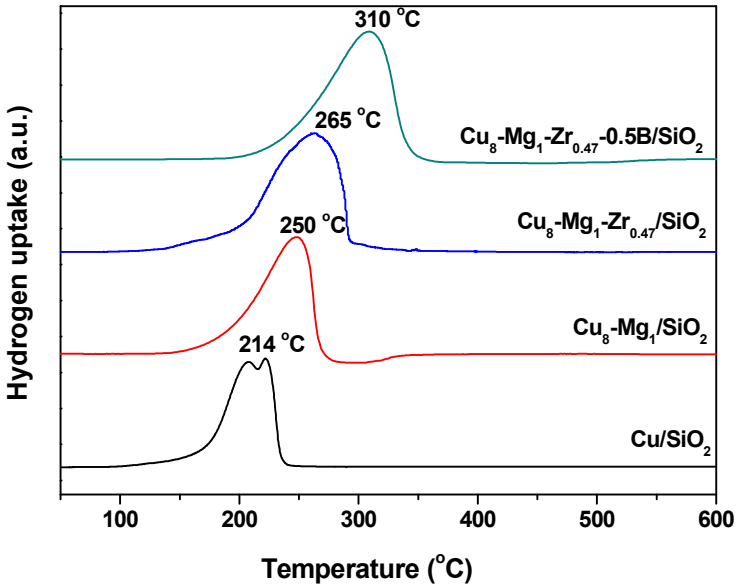

Fig. 5

View Article Online
DOI: 10.1039/C8CY00023A

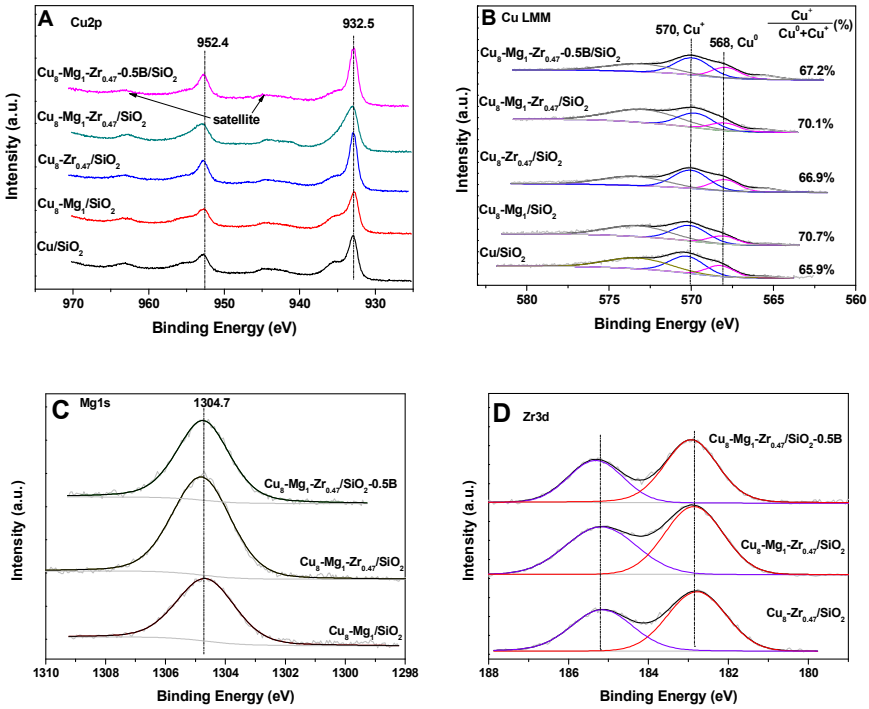

Fig. 6

View Article Online
DOI: 10.1039/C8CY00023A

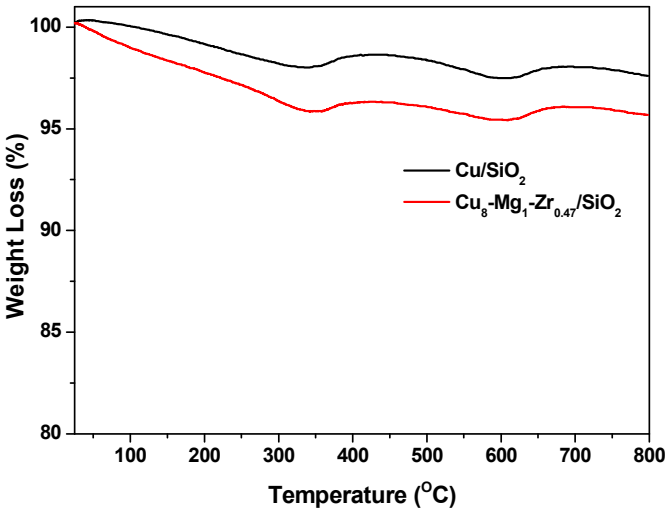

Fig. 7

View Article Online
DOI: 10.1039/C8CY00023A

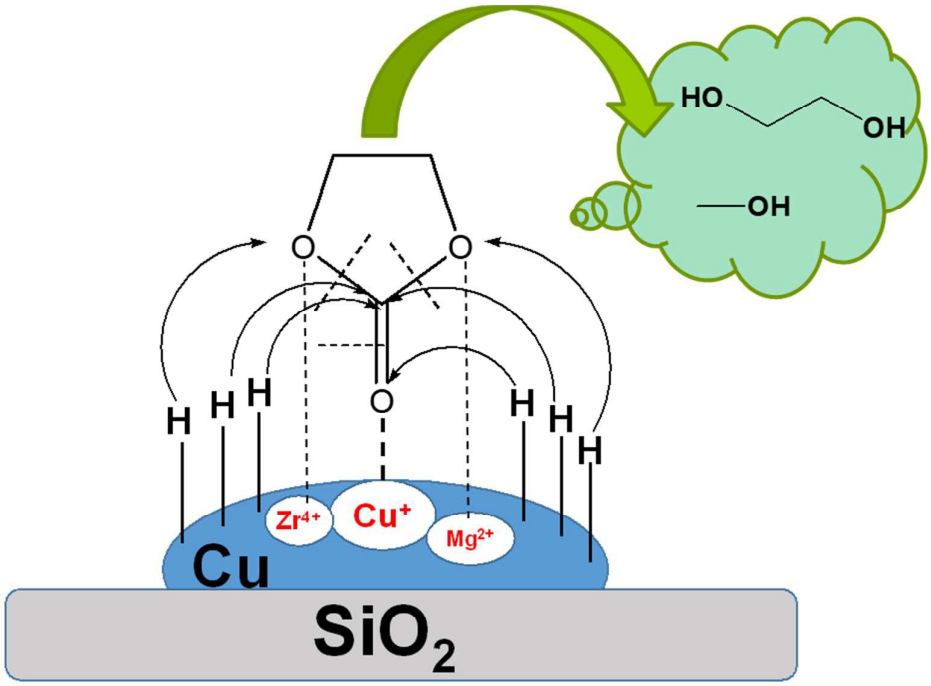

Fig. 8

View Article Online
DOI: 10.1039/C8CY00023A

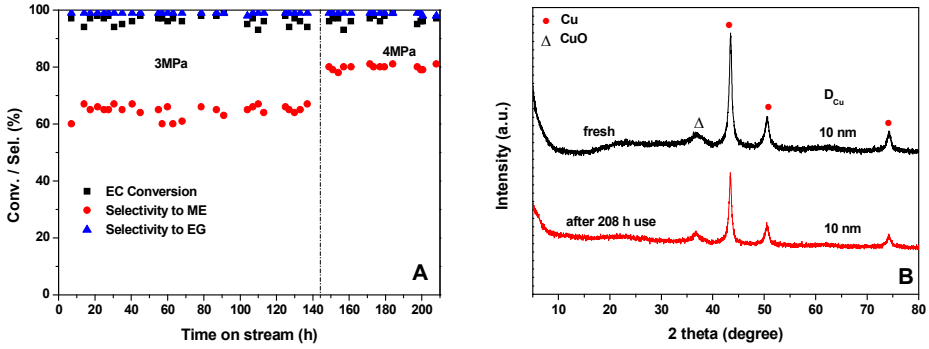

Fig. 9

View Article Online
DOI: 10.1039/C8CY00023A

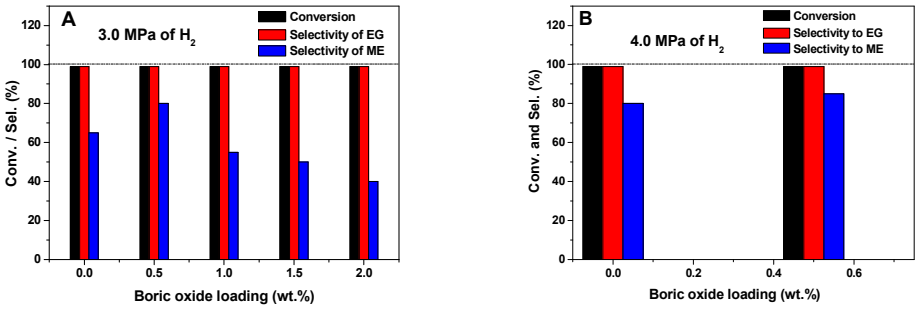

Fig. 10

View Article Online
DOI: 10.1039/C8CY00023A

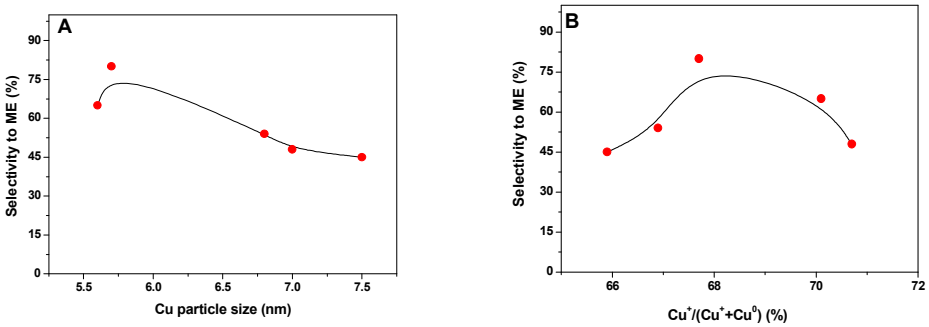

Fig. 11